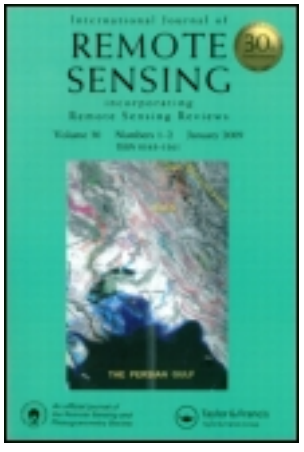

International Journal of Remote Sensing

Publication details, including instructions for authors and subscription information:
http://www.tandfonline.com/loi/tres20

Variations of surface boundary layer parameters associated with Cyclone Gonu over the Arabian Sea using QuikSCAT data

P.R. Jayakrishnan [a] & C.A. Babu [a]

[a] Department of Atmospheric Sciences, Cochin University of Science and Technology, Cochin, 682016, India

Version of record first published: 12 Dec 2012.

To cite this article: P.R. Jayakrishnan & C.A. Babu (2013): Variations of surface boundary layer parameters associated with Cyclone Gonu over the Arabian Sea using QuikSCAT data, International Journal of Remote Sensing, 34:7, 2417-2431

To link to this article: http://dx.doi.org/10.1080/01431161.2012.739734

International Journal of Remote Sensing
Vol. 34, No. 7, 10 April 2013, 2417–2431

Taylor & Francis
Taylor & Francis Group

Variations of surface boundary layer parameters associated with Cyclone Gonu over the Arabian Sea using QuikSCAT data

P.R. Jayakrishnan* and C.A. Babu

Department of Atmospheric Sciences, Cochin University of Science and Technology, Cochin 682016, India

(*Received 1 October 2011; accepted 9 July 2012*)

This study attempted to quantify the variations of the surface marine atmospheric boundary layer (MABL) parameters associated with the tropical Cyclone Gonu formed over the Arabian Sea during 30 May–7 June 2007 (just after the monsoon onset). These characteristics were evaluated in terms of surface wind, drag coefficient, wind stress, horizontal divergence, and frictional velocity using 0.5° × 0.5° resolution Quick Scatterometer (QuikSCAT) wind products. The variation of these different surface boundary layer parameters was studied for three defined cyclone life stages: prior to the formation, during, and after the cyclone passage. Drastic variations of the MABL parameters during the passage of the cyclone were observed. The wind strength increased from 12 to 22 m s^{-1} in association with different stages of Gonu. Frictional velocity increased from a value of 0.1–0.6 m s^{-1} during the formative stage of the system to a high value of 0.3–1.4 m s^{-1} during the mature stage. Drag coefficient varied from 1.5×10^{-3} to 2.5×10^{-3} during the occurrence of Gonu. Wind stress values varied from 0.4 to 1.1 N m^{-2}. Wind stress curl values varied from 10×10^{-7} to 45×10^{-7} N m^{-3}. Generally, convergent winds prevailed with the numerical value of divergence varying from 0 to -4×10^{-5} s^{-1}. Maximum variations of the wind parameters were found in the wall cloud region of the cyclone. The parameters returned to normally observed values in 1–3 days after the cyclone passage.

1. Introduction

The marine atmospheric boundary layer (MABL) has a key role in the transportation of moisture, momentum, and heat fluxes between the ocean and free atmosphere. Many studies have been carried out to understand the characteristics of the MABL, mainly based on oceanographic experiments such as the International Indian Ocean Expedition (IIOE), Barbados Oceanographic and Meteorological Experiment (BOMEX), Atlantic Trade Wind Experiment (ATEX), GARP Atlantic Tropical Experiment (GATE), Monsoon Experiment-77 (MONEX-77), MONEX-79, Bay of Bengal Monsoon Experiment-99 (BOBMEX-99), and Arabian Sea Monsoon Experiment (ARMEX). Holt and Sethu Raman (1987) examined the mean and turbulent structure of the MABL over the Bay of Bengal during MONEX-79. In their study, the mean wind profiles indicated the existence of a jet-like structure in the upper part of the boundary layer during break conditions. Furthermore, they reported that the wind profiles obtained during active monsoon periods do not show this wind maximum.

*Corresponding author. Email: prjayakrishnan@gmail.com

ISSN 0143-1161 print/ISSN 1366-5901 online

http://dx.doi.org/10.1080/01431161.2012.739734
http://www.tandfonline.com

The marine boundary layer processes over the tropical oceans have been studied by several investigators (Donelan and Miyake 1973; Pennell and LeMone 1974; Sommeria and LeMone 1978; LeMone 1980). Sam, Mohanty, and Satyanarayana (2003) studied the temporal evolution of the turbulent kinetic energy, sensible heat flux, latent heat flux, and the drag coefficient using radiosonde data taken from BOBMEX-99 during different epochs of the Indian summer monsoon. In their study, the characteristic features of the marine boundary layer over the Bay of Bengal during the southwest monsoon were investigated. The Tropical Ocean Global Atmosphere Coupled Ocean Atmosphere Response Experiment (TOGA COARE) was aimed at describing the coupling of the west Pacific warm pool to the atmosphere (Webster and Lukas 1992), providing an insight into the atmosphere–ocean coupling on an intra-seasonal timescale (Godfrey and Lindstorm 1989; Shinoda, Hendon, and Glick 1998). Satyanarayana, Mohanty, and Sam (1999) analysed the marine boundary layer processes in the intertropical convergence zone (ITCZ) and non-ITCZ regimes over the Indian Ocean with INDOEX IFP-99 data. From their observations, three distinct MABL regimes corresponding to three different convective zones were identified.

Marine atmospheric boundary layer parameters have been extensively investigated by many researchers in connection with different cruise expeditions over both the Arabian sea and the Bay of Bengal (Sethu Raman and Raynor 1975; Garrat 1977; Manghnani et al. 2000; Bhat et al. 2002; Subrahmanyam and Ramachandran 2003a, 2003b; Joseph et al. 2007).

Subrahamanyam and Ramachandran (2003) analysed the structural characteristics of the marine–atmospheric boundary layer and associated dynamics over the central Arabian Sea during the INDOEX IFP-99 campaign. The analysis of thermodynamic variable profiles revealed a double mixed-layer structure over the Central Arabian Sea region. Bhat (2003) examined the salient features of the atmosphere over the northern Bay of Bengal during BOBMEX-99. Their study describes the marine boundary layer parameters and their vertical variations based on the observations made from ORV Sagar Kanya in the northern Bay of Bengal during July–August of 1999, which includes both the active and weak phases of the monsoon. Ramana et al. (2000) made a measurement of air–sea parameters and estimated sensible and latent heat fluxes by the inertial dissipation technique over the southern Bay of Bengal. Nagar, Dhakate, and Seetharamana (2007) investigated the evolutionary features of the dynamic and thermodynamic characteristics of the marine atmosphere over the southeast Arabian Sea prior to the onset of the monsoon over Kerala during ARMEX-2003. Hamza, Babu, and Sabin (2007) studied the characteristics of the boundary layer parameters over the Arabian Sea and the Bay of Bengal using Quick Scatterometer (QuikSCAT) data. They analysed the variations of surface wind, drag coefficient, frictional velocity, and wind stress curl on a seasonal basis. Mahrt and Ek (1993) analysed the spatial variability of turbulent flux and roughness length over a heterogeneous surface using flight data collected during clear sky days and found that the effective roughness length was about 1 m.

In this study, we further investigate the MABL characteristics during the formation of Cyclone Gonu over the Arabian Sea using QuikSCAT data. The parameters studied include wind speed, drag coefficient distribution, wind stress, wind stress curl, horizontal divergence, and frictional velocity.

It is important to study the various surface boundary layer parameters over the ocean during the occurrence of different weather systems such as cyclones. There are *in situ* observations made over the ocean such as from moored buoys, cruise expeditions, XBTs, etc., which help us to understand the features of the marine boundary layer. But these *in situ* observations are limited to specific areas and also are available only during specific time periods. Owing to the advent of satellite observations, we are able to collect data over

the global oceans. There may not be any available *in situ* observations associated with the passage of a cyclone over the Arabian Sea, but QuikSCAT data are available, which provide the necessary surface boundary layer information for the system. Our main objective of this study was to quantify the variations in surface boundary layer parameters associated with a cyclone passage over the Arabian Sea using QuikSCAT data. No such studies have been carried out during the presence of such a weather system over the Arabian Sea to quantify the changes in the marine boundary layer. So, it is important to carry out such an investigation that will give rise to an understanding of the surface–marine boundary layer during the occurrence of a cyclone.

2. Data and methodology

This study utilizes 0.5° × 0.5° resolution QuikSCAT data measured by the SeaWinds scatterometer onboard the QuikSCAT satellite of the National Aeronautics and Space Agency (NASA) (Wentz 1986; Patoux and Brown 2001). The wind products are zonal and meridional wind speed, drag coefficient distribution, wind stress, wind stress curl, horizontal divergence, and frictional velocity. The raw data, supplied by JPL/PO.DAAC (Level 2B data; available at: ftp://ftp.ifremer.fr/ifremer/cersat/products/gridded/mwf-quikscat/data/daily/2007/), are analysed on a 0.5° × 0.5° global grid over various averaging time periods and are provided by IFREMER/CERSAT.

The scatterometer was designed to observe wind vectors with an accuracy of 20° in direction and 2 m s^{-1} in speed, and a spatial resolution of 25 km. This high-resolution data can be used to investigate different MABL parameters over oceanic regions, as it is very difficult to get data from field experiments. Goswami and Rajagopal (2004) made a comparison between the QuikSCAT wind and *in situ* observations obtained from various research cruises and found that the data set shows less bias with the *in situ* observations. Hence, the surface wind obtained from QuikSCAT is reliable for the computation of marine–atmospheric boundary layer parameters.

$$\text{Drag coefficient } c_{\mathrm{d}} = \tau/\rho u^2 \tag{1}$$

and

$$\text{Frictional velocity } u^* = \sqrt{\tau/\rho}, \tag{2}$$

where τ is the wind stress, c_{d} is the drag coefficient, ρ is the density of air, and u is the wind velocity at the 10 m level (Arya 2001).

For the analysis of the daily variation of marine–atmospheric boundary layer parameters associated with the low-pressure system, a special type of Hovmoller diagram is used in this study. The variation of the parameters at the centre of the low-pressure system can be evaluated using the diagram.

This study analysed the variation of surface boundary layer parameters associated with the centre of the low-pressure system for 13 days (from 26 May to 7 June 2007). The centre of low pressure was determined by identifying the minimum value of outgoing longwave radiation (OLR) during the period from 26 May to 1 June 2007, and by using the storm track information for the period from 2 to 7 June 2007. The OLR data are obtained from the NOAA site: http://www.esrl.noaa.gov/psd/data/gridded/data.interp_OLR.html.

The track information is based on the combination of satellite and radar data, and it is available from the Hurricane Data Centre site: http://weather.unisys.com/hurricane/n_indian/2011/index.html.

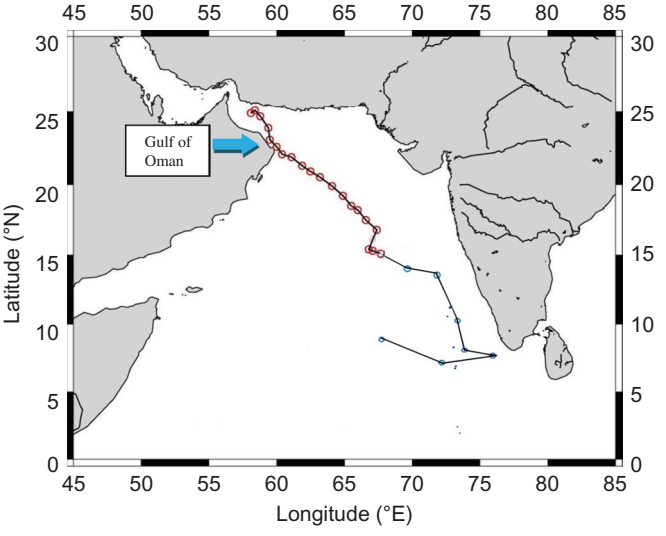

Figure 1. Track of Cyclone Gonu.

Figure 1 shows the track of the system for the entire study period, in which blue circles represent the daily location of the system before it intensifies into a cyclone and red circles represent it for the cyclone on a six-hourly basis.

3. Results and discussions

This study reports surface MABL parameters associated with the passage of Cyclone Gonu, one of the strongest tropical cyclones on record in the Arabian Sea. Actually, the monsoon onset surge over the Arabian Sea intensified into a low-pressure system and subsequently intensified into a cyclone, named as Gonu. To bring out the MABL parameters associated with the evolution of the system, we made a detailed analysis for the period from 26 May to 7 June 2007 (2 days prior to the formation of the system and until its landfall) utilizing the QuikSCAT data set. We analysed the data from 31 May to 6 June in order to understand the variation associated with different stages of the cyclone. On the basis of wind speed at the wall cloud region of the system, we identified three stages of the cyclone: the formative stage on 2 June, the mature stage on 4 June, and the dissipation stage on 6 June. The MABL parameters at the centre of the system during the different system stages are discussed.

3.1. Normal values of the parameters as inferred from the 5-year composite

Figure 2 shows the 5-year composite of surface–marine boundary layer parameters during the period from 26 May to 7 June for the years 2002–2006. From Figure 2(*a*), the normal value of wind speed over the Arabian Sea is found to be between 8 and 12 m s^{-1} with a maximum of 14 m s^{-1}. The normal value of wind stress ranges between 0.2 and 0.4 with a maximum of 0.8 N m^{-2} (Figure 2(*b*)). From Figure 2(*c*), the normal value of horizontal divergence is found to be between 5–10 $\times$ 10^{-6} s^{-1} with a maximum of 20 $\times$ 10^{-6} s^{-1} over the Arabian Sea. The wind stress curl value is between 0 and 2 $\times$ 10^{-7} N m^{-3} with a maximum of 15 $\times$ 10^{-7} N m^{-3} (Figure 2(*d*)). The drag coefficient has a normal value between 1 and 1.5 $\times$ 10^{-3} and the frictional velocity varies between 0.4 and 0.5 m s^{-1} (Figures 2(*e*) and (*f*)).

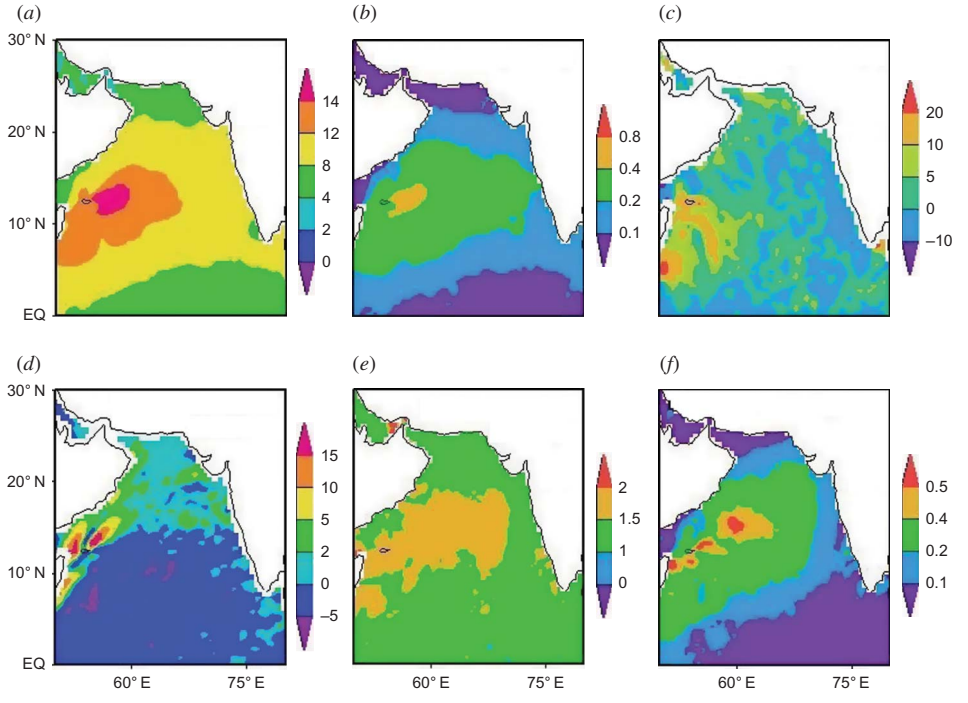

Figure 2. Five-year composites of parameters: (*a*) wind speed (m s^{-1}), (*b*) wind stress (N m^{-2}), (*c*) horizontal divergence ($\times 10^{-6}$ s^{-1}), (*d*) wind stress curl ($\times 10^{-7}$ N m^{-3}), (*e*) drag coefficient ($\times 10^{-3}$), and (*f*) frictional velocity (m s^{-1}).

3.2. *Organized convection associated with the system inferred from OLR*

Figure 3 represents OLR from 27 May to 7 June during different stages of the low-pressure system. Low OLR values indicate the presence of intense organized convection. A small patch of organized convection was seen near the southwest peninsula of India on 27 May and it intensified further into a monsoon onset surge. It became a well-marked low in the southeast Arabian Sea on 29 May. The low-pressure system intensified further on 1 June to become a depression first and then a deep depression. On 2 June, it became a cyclone (formative stage) and intensified into a severe cyclone on 4 June (mature stage). Intense organized convection was observed from 2 June to 5 June in the location of the Gonu system with an OLR value of less than 120 W m^{-2}. Landfall occurred over the Oman coast on 6 June. After the dissipation of the system, revival of the monsoon took place in the equatorial region on 7 June.

3.3. *Variation of surface boundary layer parameters*

3.3.1. *Wind speed*

On 1 June, wind speed values were less than 10 m s^{-1} over the region of the formation of the cyclone. Figure 4 shows the spatial distribution of surface wind speed during the formative, mature, and dissipating stages of Cyclone Gonu. The wind speed was around 12–14 m s^{-1} on 2 June 2007 (formative stage), and increased to 16–18 m s^{-1} on 3 June and further increased to 20–22 m s^{-1} on 4 June (mature stage). Landfall occurred on 6 June and wind speed decreased quickly. The wind speed became 4–8 m s^{-1} over the region of the formation of the cyclone and it took 1 day to return to a normal value (Figure 2(*a*)).

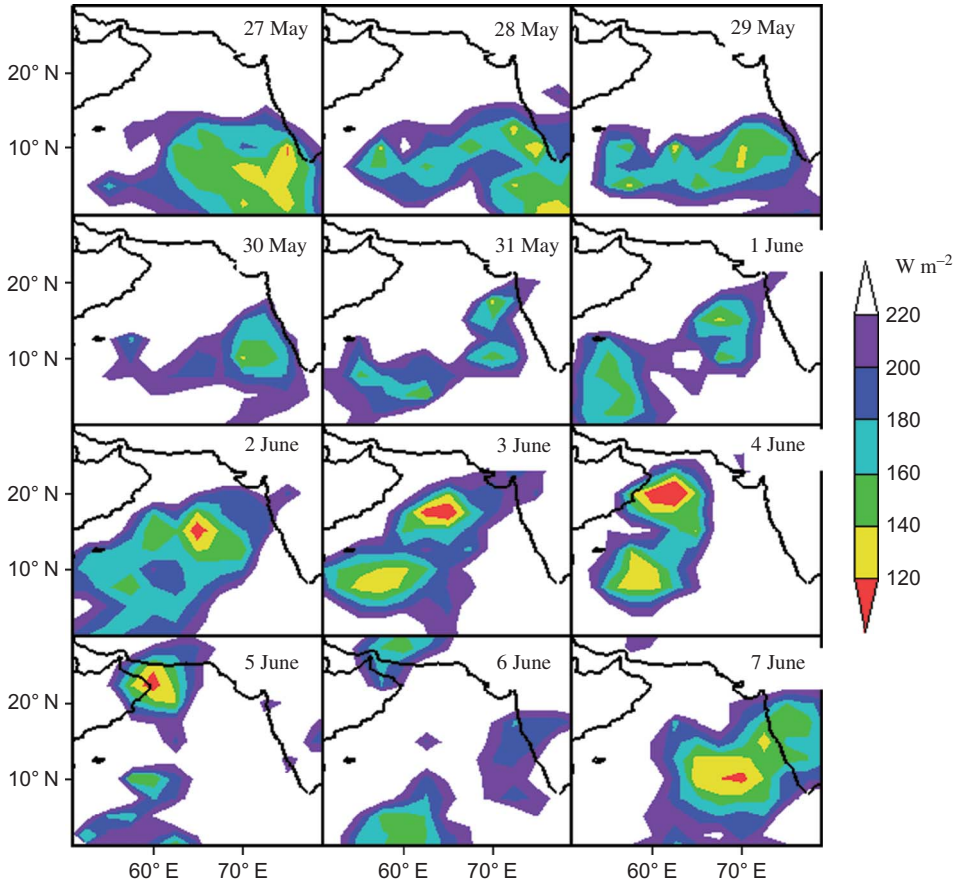

Figure 3. Outgoing longwave radiation during different stages of Cyclone Gonu.

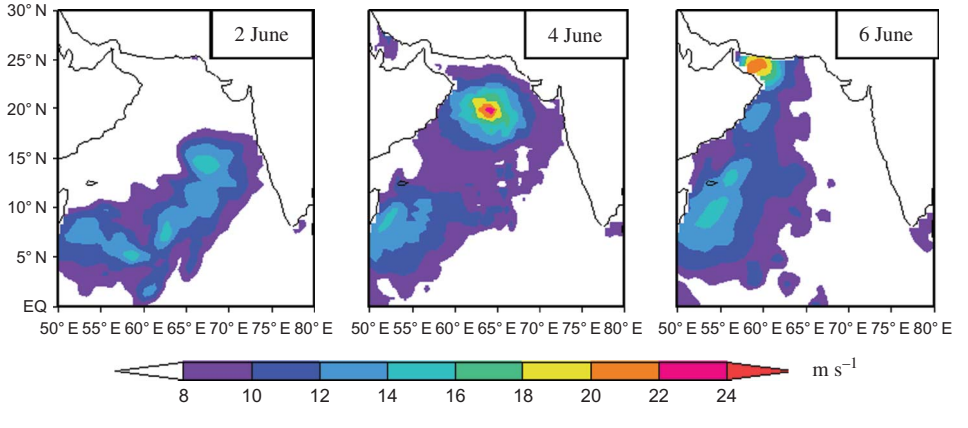

Figure 4. Surface wind speed during different stages of Cyclone Gonu.

3.3.2. *Drag coefficient*

Figure 5 depicts the variation of the drag coefficient during the three stages of the cyclone. During the formative stage, the value was found to be 1.5×10^{-3} to 2×10^{-3}. When the cyclone intensified into its mature stage, the value increased to 2.5×10^{-3} due to the increase in wind speed. The c_d values over the Arabian Sea during the presence of the system are similar to those reported by Subrahmanyam and Ramachandran (2003a, 2003b), Manghnani et al. (2000), and Bhat et al. (2002), which were derived from different *in situ* observations taken during field experiments. When the system was in its mature stage, the wind speed was more than 22 m s^{-1} and the strong wind made c_d values increase to 2.5×10^{-3} at the wall cloud region of the system. Since it is difficult to arrange *in situ* observations during the presence of severe cyclonic storms, MABL features were not reported earlier from the Arabian Sea. We found that the c_d values closely follow the strength of the wind and it took 1 day for them to return to the normal range (Figure 2(*e*)).

3.3.3. *Wind stress*

Wind stress mainly depends on surface winds. When the system originated as a well-marked low in the East Arabian Sea on 28 May, the wind stress values over the region were more than 0.1 N m^{-2}. These values were in the same range as those reported by Hellerman and Rosenstein (1983) for the mean monthly wind stress over the world's oceans. They reported a wind stress value of 0.1 N m^{-2} over the Arabian Sea. On 1 June (before the development of the low-pressure system into a cyclone), the values in the vicinity of the system increased due to strengthening of the wind. During the formative stage of the cyclone (2 June), the value of wind stress was 0.4–0.5 N m^{-2} as shown in Figure 6. The value increased further as the system intensified, and in the mature stage of the cyclone (4 June), the value became 1–1.2 N m^{-2}. These values were in agreement with the wind stress values derived from buoy data for a cyclone formed in the Bay of Bengal, as reported by Joseph et al. (2007). By landfall, the wind stress value decreased due to the decrease in wind speed. The wind stress values before the intensification of the system were small, as the wind was feeble. These values were similar to the wind stress values derived from *in situ* observations based on field experiments (Manghnani et al. 2000). It took 3 days for the retrieval of wind stress values in the region of the system centre to become normal (Figure 2(*b*)), even

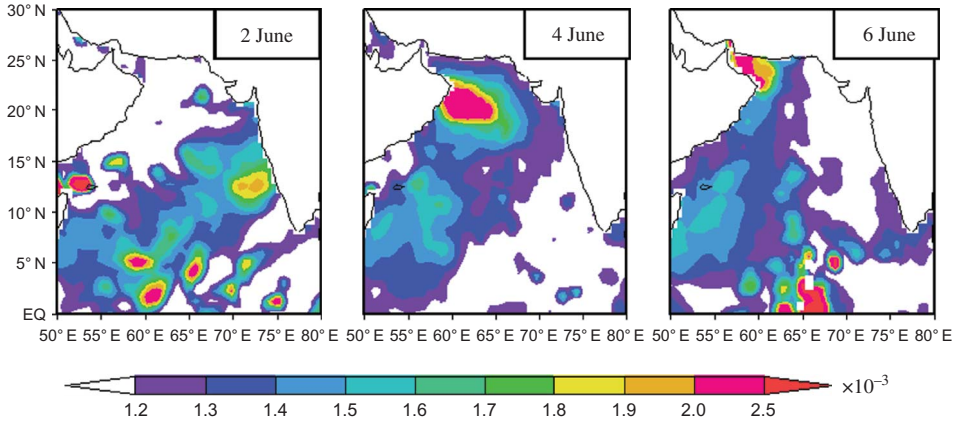

Figure 5. Drag coefficient during different stages of Cyclone Gonu.

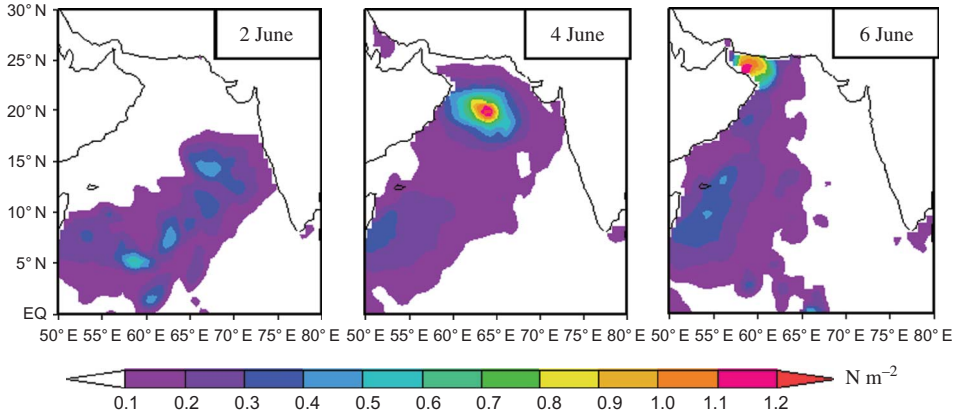

Figure 6. Wind stress during different stages of Cyclone Gonu.

though wind strength decreased immediately as the system moved away from the location. Murtugudde, McCreary, and Antonio (2000) examined the oceanic processes associated with anomalous events in the Indian Ocean utilizing NCEP data. They also found that the wind stress vectors were in the range of 0.1–0.3 N m^{-2} over the Indian Ocean.

3.3.4. Wind stress curl

Figure 7 depicts wind stress curl over the Arabian Sea during different stages of the low-pressure system. On 31 May (when the system was a depression), the value was 5×10^{-7} N m^{-3} over the region of the formation of the system. It suddenly increased to 15×10^{-7} N m^{-3} on 1 June when the system intensified into a deep depression. When it became a cyclone (formative stage) on 2 June, the value of wind stress curl was 20×10^{-7} N m^{-3}. During the mature stage (4 June), the value again increased to more than 45×10^{-7} N m^{-3} over a small area at the centre of the system surrounded by slightly lower values (30×10^{-7} N m^{-3}). The wind stress curl also depends on the wind speed. As the wind speed decreased due to landfall of the system, the wind stress curl value over the Arabian Sea returned to 5×10^{-7} N m^{-3} on 7 June. This value is in the same range of values presented in the atlas by Hastenrath and Lamb (1979). Trenberth, Large, and Olson (1990) also found a wind stress curl value of 2×10^{-7} N m^{-3} over the southern Indian Ocean. On the basis of the QuikSCAT data, Milliff et al. (2004) reported that high wind stress curl values occur between 10×10^{-7} N m^{-3} and 20×10^{-7} N m^{-3} over the Indian Ocean region due to strong surface winds associated with the presence of organized convection during the passage of the ITCZ. It took 1–2 days for the high wind stress curl values to return to normal (Figure 2(*d*)).

3.3.5. Horizontal divergence

Generally, in the presence of low-pressure systems, the horizontal divergence value is negative. This is known as wind convergence. Figure 8 shows the variation of horizontal divergence in different stages of the low-pressure system. During the formative stage, the value was -3.5×10^{-5} s^{-1}. This indicates the presence of wind convergence over the Southeast Arabian Sea when the low-pressure system was intensified into a cyclone.

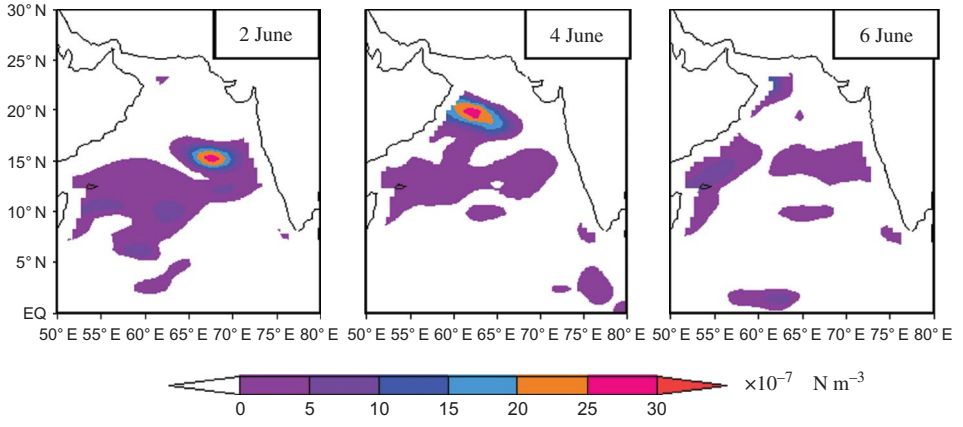

Figure 7. Wind stress curl during different stages of Cyclone Gonu.

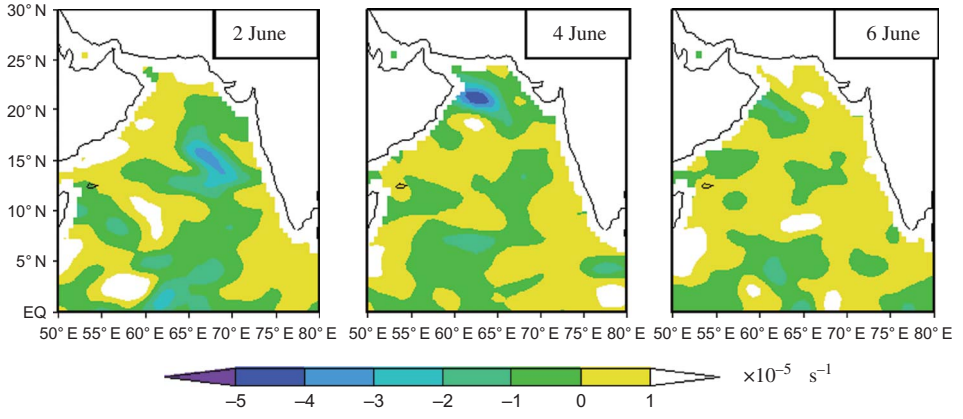

Figure 8. Horizontal divergence during different stages of Cyclone Gonu.

Further, the convergence increased to 4.5×10^{-5} s^{-1} when the system became mature. During landfall, the convergence decreased to 0.5×10^{-5} s^{-1} as the cyclonic circulation weakened. The cyclonic circulation took 1–2 days for weakening in the region of the low-pressure system. Hence, the horizontal divergence value came back to the normal value (Figure 2(*c*)) (between -0.5×10^{-5} and 0.5×10^{-5} s^{-1}) within 2 days. Wood et al. (2009) analysed the diurnal cycle of surface divergence over the global oceans and reported a convergence value of 0.2×10^{-5} s^{-1} over the tropics.

3.3.6. Frictional velocity

Figure 9 shows the variation of frictional velocity during different stages of the cyclone. On 1 June, the frictional velocity was 0.1 m s^{-1}. During the formative stage of the system (2 June), the value was 0.4–0.5 m s^{-1}. During its mature stage, the value was found to be 0.9–1.4 m s^{-1}. On 7 June, the frictional velocity value decreased abruptly to 0.4 m s^{-1} as the surface wind strength decreased due to landfall of the system. The values decreased further to 0.1 m s^{-1} in the region of the system as the wind strength became normal when the system completely dissipated. The normal value for frictional velocity is shown in Figure 2(*f*). The frictional velocity values are similar to that reported by Hamza, Babu, and Sabin (2007)

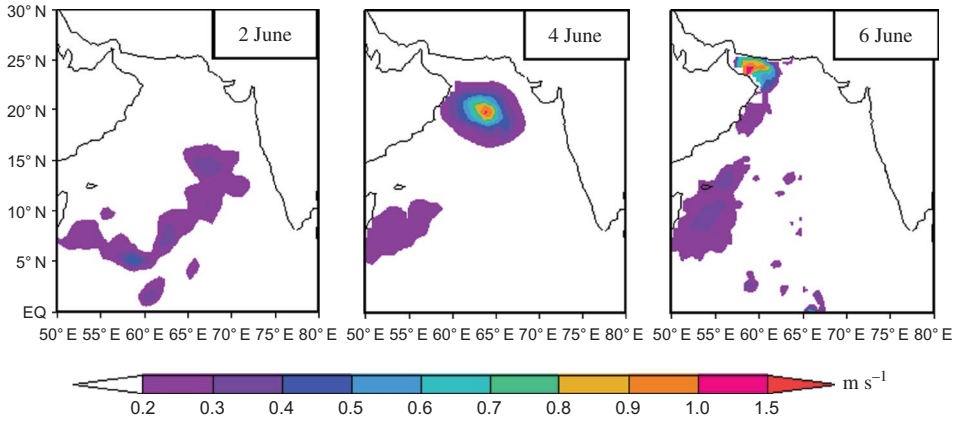

Figure 9. Frictional velocity during different stages of Cyclone Gonu.

in their study on the seasonal variation of frictional velocity over the Arabian Sea and the Bay of Bengal.

3.3.7. *Observed wind vector changes and MABL parameters*

The data procured from IFREMER contain the following surface-wind derived parameters: zonal and meridional components of wind, zonal and meridional components of wind stress, wind stress curl, and horizontal divergence. The method of computation of different wind-derived parameters is described in the manual provided by IFREMER/CERSAT (NASA 2000). All of these MABL parameters are derived from the basic dynamic equations involving zonal and meridional components of wind (Hsu 1988). Hence, it is clear that the observed changes in surface MABL parameters are caused mainly by the variations in surface-wind components. The drastic variation in wind associated with the intensification and movement of the system is responsible for the abrupt changes in surface MABL. The cyclonic vorticity and convergent wind associated with the system are responsible for the development of strong wind-stress curl and changes in other surface–marine boundary layer parameters.

3.3.8. *Daily variation of boundary layer parameters during Cyclone Gonu*

Figure 10 shows the daily variation of different parameters during Cyclone Gonu. Figure 10(*a*) shows the variation of wind stress during different stages of the cyclone. It varied from 0.4 N m^{-2} to 0.8 N m^{-2} during the formative stage. Then, it increased to 1.4 N m^{-2}, and thereafter it decreased rapidly to 1.2 N m^{-2} and to 0.4 N m^{-2} during landfall. Figure 10(*b*) shows the variation of surface wind speed during the occurrence of the cyclone. The wind speed increased from 12 to 18 m s^{-1} during the formative stage and further increased from 18 to 22 m s^{-1} during its mature stage. It gradually decreased from 18 to 12 m s^{-1} due to landfall. The drag coefficient variation was found to be irregular (Figure 10(*c*)). It has a value of 2.0×10^{-3} during the formative stage and decreased to 1.5×10^{-3} and then increased to 2.5×10^{-3} during landfall. The wind stress curl has a value 10×10^{-7} to 15×10^{-7} N m^{-3} during the formative stage (Figure 10(*d*)). During the mature stage, the value increased up to 45×10^{-7} N m^{-3}. During landfall, it again decreased to 5×10^{-7} to 10×10^{-7} N m^{-3}. A horizontal divergence value of

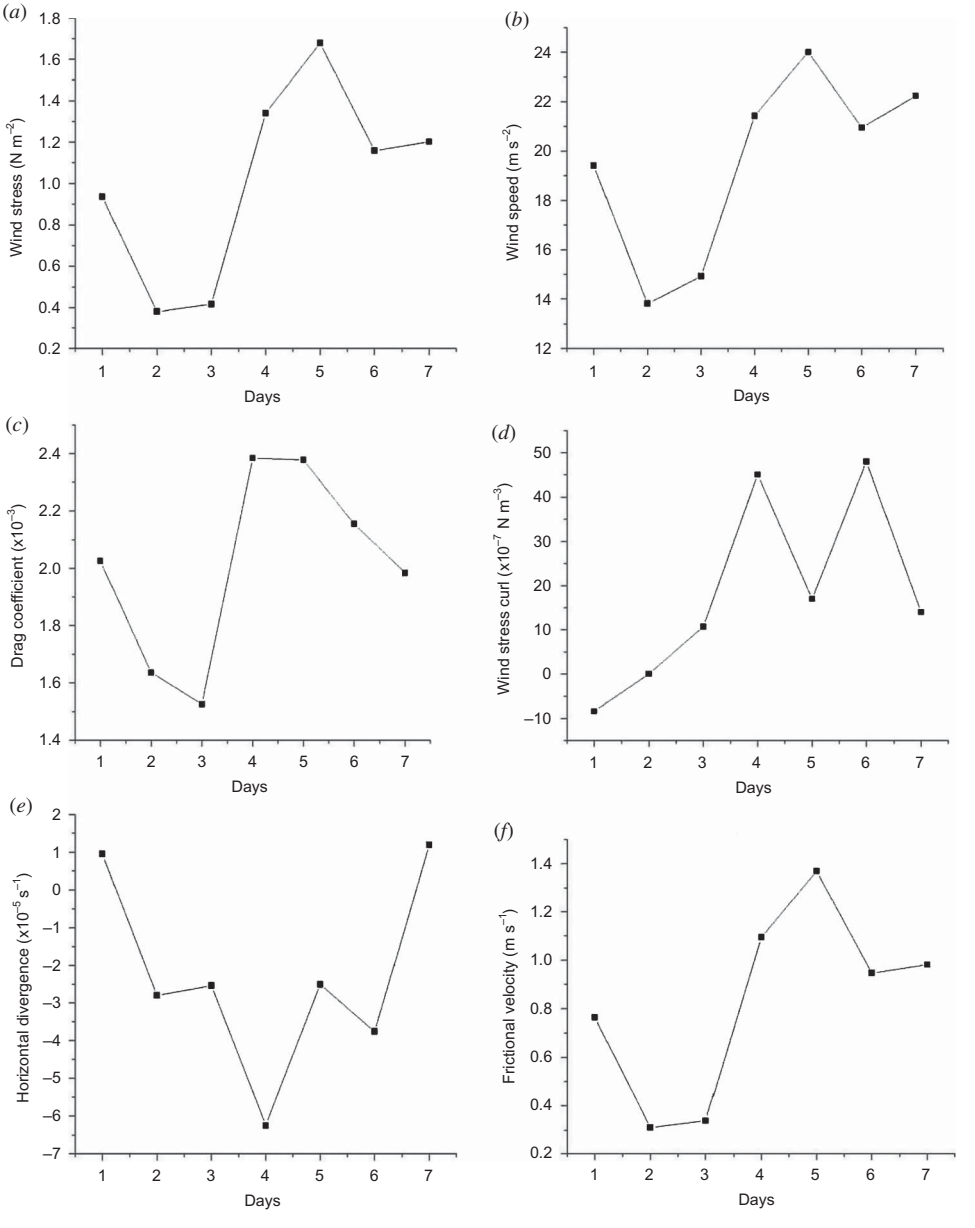

Figure 10. Variation of different MABL parameters during 31 May–6 June observed at the centre of the cyclone.

-2×10^{-5} s^{-1} was observed during the formative stage (Figure 10(*e*)). Then, the wind convergence increased to -6×10^{-5} s^{-1} during the mature stage of Cyclone Gonu. During the landfall of the system, the divergence value changed from -1×10^{-5} to 0 s^{-1}. Frictional velocity was 0.2–0.5 m s^{-1} during the formative stage (Figure 10(*f*)). An increase in value to 1.4 m s^{-1} was observed during the mature stage. Then, the value decreased to 0.2 m s^{-1} during the landfall.

3.3.9. *MABL parameters based on Hovmoller diagram*

Figure 11 represents the evolution of marine–atmospheric boundary layer parameters at different locations on the track of the system during the period from 26 May to 7 June as a Hovmoller diagram for (*a*) wind speed, (*b*) wind stress, and (*c*) wind stress curl. Maximum wind speed was 18–22 m s^{-1} during 3–4 June, when the system intensified into a severe cyclonic storm. Table 1 gives details of the corresponding 28 locations of the cyclone that were used to prepare the Hovmoller diagram. From 5 June onwards, the wind speed decreased drastically to less than 10 m s^{-1} due to landfall and dissipation of the cyclone. Wind stress also followed the same pattern of wind speed (Figure 11(*b*)). In association with high wind speed, the wind stress reached a maximum value at the centre of the cyclone with a value of 0.6 to 0.7 N m^{-2} during 3–4 June. After 5 June, it suddenly decreased due to the landfall of the cyclone. Wind stress curl values were found between 20×10^{-7} and 25×10^{-7} N m^{-3} over small regions close to the centre of the system during 1–5 June followed by small values in the other locations before 1 June and after 5 June (Figure 11(*c*)). The drag coefficient was above 2×10^{-3} at the centre of the cyclone (Figure 12(*a*)). At the time of landfall, c_d increased to 2.5×10^{-3}. Horizontal wind convergence exceeded 3×10^{-5} s^{-1} on 1 June (Figure 12(*b*)) as the system intensified. Frictional velocity also showed the same pattern of wind speed (Figure 12(*c*)). The highest value of 0.7 m s^{-1} was found during 3–4 June.

4. Conclusions

The variation of different surface boundary layer parameters over the ocean during the occurrence of Cyclone Gonu was discovered using QuikSCAT data. There have been many attempts to study the marine boundary layer using different data sets such as cruise data and buoy data. Since these types of *in situ* data are limited to some locations only, we were not able to get a continuous monitoring of the ocean surface. When there is a passage of a

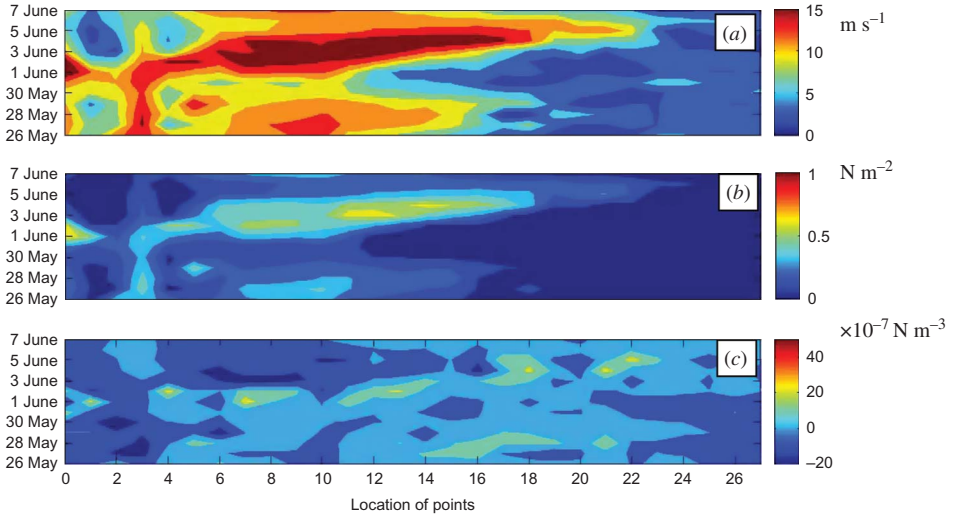

Figure 11. Hovmoller diagram representing the evolution of marine–atmospheric boundary layer parameters at different locations on the track of the system during the period from well-marked low to landfall: (*a*) wind speed, (*b*) wind stress, and (*c*) wind stress curl.

Table 1. Location and track of the cyclone as obtained from Unisys Weather.

Location number	Date (May–June 2007)	Latitude (°N)	Longitude (°E)	Time Z (GMT)	Category of cyclone
1	26	10.00	67.00	–	–
2	27	06.00	72.00	–	–
3	28	07.00	76.00	–	–
4	29	07.00	58.00	–	–
5	30	11.00	74.00	–	–
6	31	14.00	72.00	–	–
7	1	16.00	70.00	–	–
8	2	15.00	68.00	–	–
9	2	15.10	67.70	0000	Tropical storm
10	2	15.30	67.10	1200	Tropical storm
11	2	15.40	66.80	1800	Tropical storm
12	3	16.80	67.40	0600	Tropical storm
13	3	17.50	66.60	1200	Cyclone 1
14	3	18.20	66.00	1800	Cyclone 2
15	4	18.50	65.50	0000	Cyclone 4
16	4	19.20	64.90	0600	Cyclone 4
17	4	19.90	64.10	1200	Cyclone 5
18	4	20.50	63.20	1800	Cyclone 5
19	5	20.90	62.50	0000	Cyclone 4
20	5	21.30	61.90	0600	Cyclone 4
21	5	21.90	61.10	1200	Cyclone 3
22	5	22.10	60.40	1800	Cyclone 2
23	6	22.60	60.00	0000	Cyclone 1
24	6	23.10	59.50	0600	Cyclone 1
25	6	23.90	59.40	1200	Cyclone 1
26	6	24.70	58.80	1800	Tropical storm
27	7	25.10	58.40	0000	Tropical storm
28	7	24.90	58.10	0600	–

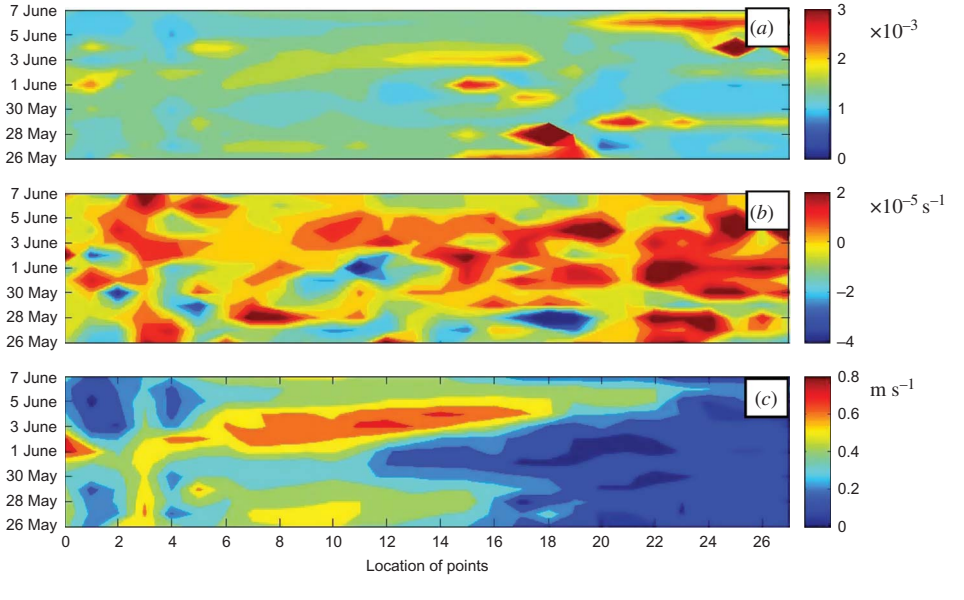

Figure 12. Hovmoller diagram representing the evolution of marine–atmospheric boundary layer parameters at different locations on the track of the system during the period from well-marked low to landfall: (*a*) drag coefficient, (*b*) horizontal divergence, and (*c*) frictional velocity.

low-pressure system such as a cyclone over the ocean surface, the surface boundary layer parameters drastically change. At the time of occurrence of such systems, there may not be any *in situ* observations to quantify the changes. Here comes the potential of satellite-derived products in monitoring severe weather systems. QuikSCAT provides a global data set of ocean surface winds, which can be used as a source for assessing surface wind characteristics over the oceanic region. This is the first study that uses QuikSCAT data for the analysis of surface wind properties during the presence of a super cyclone over the Arabian Sea. The variations of different parameters are summarized below. The wind speed varied from 12 to 20 m s^{-1} during different stages of the cyclone. The value of wind stress varied from 0.4 to 1.1 N m^{-2}. The drag coefficient varied from 1.5×10^{-3} to 3.5×10^{-3} during the occurrence of Cyclone Gonu. The wind stress curl value varied from 10×10^{-7} to 30×10^{-7} N m^{-3}. Horizontal divergence varied from 0 to -4×10^{-5} s^{-1}. The value of frictional velocity ranged from 0.2 to 0.8 m s^{-1} during different stages of the cyclone. The intensity of the cyclone is reflected in the daily variation of the parameters and propagation of the system during different stages. Evolution of various marine–atmospheric boundary layer parameters during the formation of a severe cyclonic storm at different locations on the track of the system were brought out using a Hovmoller diagram. It is noted that the parameters return to the normal range within 3 days of the passage of the cyclone.

Acknowledgements

The first author is thankful to CSIR, New Delhi, for providing the Research Fellowship. The authors acknowledge the QuikSCAT data obtained from CERSAT/IFREMER.

References

Arya, S. P. 2001. *Introduction to Micrometeorology*. 2nd ed., 224 pp. San Diego, CA: Academic Press.

Bhat, G. S. 2003. "Salient Features of the Atmosphere Observed Over the North Bay of Bengal during BOBMEX." *Proceedings of Indian Academy of Science (Earth and Planeary Sciences)* 112: 131–46.

Bhat, G. S., M. A. Thomas, J. V. S. Raju, and C. P. Chandrasekhara. 2002. "Surface Characteristics Observed Over the Central Tropical Indian Ocean during INDOEX IFP99." *Boundary-Layer Meteorology* 106: 263–81.

Donelan, M., and M. Miyake. 1973. "Spectra and Fluxes in the Boundary Layer of the Trade Wind Zone." *Journal of Atmospheric Science* 30: 444–64.

Garrat, J. R. 1977. "Review Off the Drag Coefficients Over the Oceans and Continents." *Monthly Weather Review* 105: 915–29.

Godfrey, J. S., and E. J. Lindstorm. 1989. "On the Heat Budget of Equatorial West Pacific Surface Mixed Layer." *Journal of Geophysical Research* 94: 8007–17.

Goswami, B. N., and E. N. Rajagopal. 2004. "Indian Ocean Surface Winds from NCMRWF Analysis as Compared to QuikSCAT and Moored Buoy Winds." *Proceedings of Indian Academy of Sciences (Earth and Planetary Sciences)* 112: 61–7.

Hamza, V., C. A. Babu, and T. P. Sabin. 2007. "Characteristic Study of the Boundary Layer Parameters Over the Arabian Sea and Bay of Bengal Using the QuikSCAT Dataset." *Advances in Atmospheric Sciences* 24: 631–43.

Hastenrath, S., and P. J. Lamb. 1979. *Climatic Atlas of the Indian Ocean. Part I: Surface Climate and Atmospheric Circulation*. Madison: University of Wisconsin Press.

Hellerman, S., and M. Rosenstein. 1983. "Normal Monthly Mean Wind Stress Over the World Ocean with Error Estimates." *Journal of Physical Oceanography* 4: 145–67.

Holt, T., and S. Sethu Raman. 1987. "The Study of Mean Boundary Layer Structures Over the Arabian Sea and the Bay of Bengal During Active and Break Monsoon Periods." *Boundary-Layer Meteorology* 38: 73–94.

Hsu, S. A. 1988. *Coastal Meteorology*, 96–123. San Diego, CA: Academic Press.

Joseph, J. K., A. N. Balchand, P. V. Hareeshkumar, and G. Rajesh. 2007. "Inertial Oscillation Forced by the September 1997 Cyclone in the Bay of Bengal." *Current Science* 92: 790–4.

LeMone, M. A. 1980. "The Marine Boundary Layer." Workshop on the Planetary Boundary Layer, Boulder. *American Meteorological Society*, 182–246.

Mahrt, L., and M. Ek. 1993. "Spatial Variability of Turbulent Fluxes and Roughness Lengths in Hapex-Mobilhy." *Boundary-Layer Meteorology* 65: 381–400.

Manghnani, V., S. Sethu Raman, D. S. Niyogi, V. Parameswara, J. M. Morrison, S. V. Ramana, and J. V. S. Raju. 2000. "Marine Boundary-Layer Variability Over the Indian Ocean During INDOEX (1998)." *Boundary-Layer Meteorology* 97: 411–30.

Milliff, R. F., J. Morzel, D. B. Chelton, and M. H. Freilich. 2004. "Wind Stress Curl and Wind Stress Divergence Biases from Rain Effects on QUIKSCAT Surface Wind Retrievals." *Journal of Atmospheric and Oceanic Technology* 21: 1216–31.

Murtugudde, R., J. P. McCreary Jr, and J. B. Antonio. 2000. "Oceanic Processes Associated with Anomalous Events in the Indian Ocean with Relevance to 1997–1998." *Journal of Geophysical Research* 105, C2: 3295–306.

Nagar, S. G., A. R. Dhakate, and P. Seetharamana. 2007. "Evolutionary Features of Marine Atmospheric Boundary Layer (MABL) Over the Arabian Sea and the Onset of Monsoon Over Kerala During ARMEX-2003." *Pure Applied Geophysics* 164: 1861–80.

NASA Quick Scatterometer. 2000. QuikSCAT Science Data Product, User's Manual, Overview & Geophysical Data Products, Version 2.0-Draft, Jet Propulsion Laboratory, California Institute of Technology, Doc. D–18053.

Patoux, J., and R. A. Brown. 2001. "A Scheme for Improving Scatterometer Surface Wind Fields." *Journal of Geophysical Research* 106: 23995–4005.

Pennell, W. T., and M. A. LeMone. 1974. "An Experimental Study of Turbulence Structure in the Fair-Weather Boundary Layer." *Journal of Atmospheric Science* 31: 1308–23.

Ramana, M. V., K. Senguptha, G. S. Bhat, S. Ameenulla, and J. V. S. Raju. 2000. "Inertial Dissipation Flux Measurements Over South Bay of Bengal during BOBMEX – Pilot Experiment." *Proceedings of Indian Academy of Sciences (Earth and Planetary Sciences)* 109: 239–47.

Sam, N. V., U. C. Mohanty, and A. N. V. Satyanarayana. 2003. "Simulation of Marine Boundary Layer Characteristics Using a 1-D PBL Model Over the Bay of Bengal during BOBMEX-99." *Proceedings of Indian Academy of Sciences (Earth and Planetary Sciences)* 112: 185–204.

Satyanarayana, A. N. V., U. C. Mohanty, and N. V. Sam. 1999. "A Study on Marine Boundary Layer Processes in the ITCZ and Non-ITCZ Regimes Over Indian Ocean with INDOEX IFP-99 Data." *Current Science* 76: 890–7.

Sethu Raman, S., and G. S. Raynor. 1975. "Surface Drag Coefficient Dependence on the Aerodynamic Roughness of the Sea." *Journal of Geophysical Research* 80: 49.

Shinoda, T., H. H. Hendon, and J. D. Glick. 1998. "Intra-Seasonal Sea Surface Temperature Variability in the Tropical Pacific and Indian Ocean." *Journal of Climate* 11: 1685–702.

Sommeria, G., and M. A. LeMone. 1978. "Direct Testing of a Three-Dimensional Model of the Planetary Boundary Layer Against Experimental Data." *Journal of Atmospheric Science* 35: 25–39.

Subrahmanyam, D. B., and R. Ramachandran. 2003a. "Structural Characteristics of Marine Atmospheric Boundary Layer and Its Associated Dynamics Over the Central Arabian Sea during INDOEX, IFP-99 Campaign." *Current Science*, 85: 1334–40.

Subrahmanyam, D. B., and R. Ramachandran. 2003b. "Wind Speed Dependence of Air–Sea Exchange Parameters Over the Indian Ocean during INDOEX, IFP-99." *Annales Geophysicae* 21: 1667–79.

Trenberth, K. E., W. G. Large, and J. G. Olson. 1990. "The Mean Annual Cycle in Global Ocean Wind Stress." *Journal of Physical Oceanography* 20: 1742–60.

Webster, P. J., and R. Lukas. 1992. "TOGA COARE: The Coupled Ocean–Atmosphere Response Experiment." *Bulletin of American Meteorological Society* 3: 1377–426.

Wentz, F. J. 1986. Users manual SEASAT scatterometer wind vectors. RSS Technical Report 081586, 21. Santa Rosa, CA: Remote Sensing Systems.

Wood, R., M. Kohler, R. Bennartz, and C. O'Dell. 2009. "The Diurnal Cycle of Surface Divergence Over the Global Oceans." *Quarterly Journal of the Royal Meteorological Society*. doi:10.1002/qj.451.